nature geoscience

ARTICLES

PUBLISHED ONLINE: 16 DECEMBER 2012 | DOI: 10.1038/NGEO1669

Primary surface ruptures of the great Himalayan earthquakes in 1934 and 1255

S. N. Sapkota[1], L. Bollinger[2]*, Y. Klinger[3], P. Tapponnier[4], Y. Gaudemer[3] and D. Tiwari[1]

It is unclear where plate boundary thrusts generate giant rather than great earthquakes. Along the Himalayas, the source sizes and recurrence times of large seismic events are particularly uncertain, since no surface signatures were found for those that shook the range in the twentieth century. Here we challenge the consensus that these events remained blind and did not rupture the surface. We use geomorphological mapping of fluvial deposits, palaeo-seismological logging of river-cut cliffs and trench walls, and modelling of calibrated ^{14}C ages, to show that the M_w 8.2 Bihar–Nepal earthquake on 15 January 1934 did break the surface: traces of the rupture are clear along at least 150 km of the Main Frontal Thrust fault in Nepal, between 85° 50′ and 87° 20′ E. Furthermore, we date collapse wedges in the Sir Valley and find that the 7 June AD 1255 earthquake, an event that devastated Kathmandu and mortally wounded the Nepalese King Abhaya Malla, also ruptured the surface along this stretch of the mega-thrust. Thus, in the past 1,000 years, two great earthquakes, 679 years apart, rather than one giant eleventh-century AD event, contributed to the frontal uplift of young river terraces in eastern Nepal. The rare surface expression of these earthquakes implies that surface ruptures of other reputedly blind great Himalayan events might exist.

Although Himalayan earthquakes threaten millions of people, assessing seismic hazard along the range's Main Frontal Thrust (MFT) and understanding its seismic behaviour have proved frustratingly difficult. In contrast with the spectacular breaks produced by recent, $M \geq 7.5$, Asian thrust earthquakes[1–4], and despite the prominence of fault scarps in the Siwaliks and lesser Himalayas[5,6], no seismic surface rupture was observed on the Himalayan front during $M \sim 8$ nineteenth and twentieth century events. In trenches across the MFT trace, only much older events, and no multi-event sequences have been exposed[7–9]. The return time of great Himalayan earthquakes has thus remained uncertain. Moreover, the large slip deficit revealed by recent Global Positioning System measurements[10,11], compounded by loosely constrained inferences on the source lengths and maximum magnitudes of ancient earthquakes[7–9], has been taken to raise the odds of events greater (as high as M9?) than those instrumentally recorded[11,12].

Perhaps the most puzzling paradox is that, in spite of their relatively recent occurrence and sizes, the $M \sim 8$ Kangra (1905) and Bihar–Nepal (1934) earthquakes (Fig. 1a,b) produced no surface rupture[7,13,14]. To test whether such ruptures, essential for palaeo-seismological reconstructions, might have been overlooked both at the time of the events and in recent trenches, we investigated in detail the Quaternary geomorphology of the region between Bardibas (Ratu River valley) and the eastern border of Nepal, within the zone of strongest shaking in 1934. We targeted the area east of the Mahara River (Fig. 1), where evidence for active faulting and uplift is clearest on topographic maps, satellite images and aerial photos. Here the MFT divides into right-stepping strands with sharp geomorphic traces[6,15] marked by steep cumulative escarpments (Fig. 1c and Supplementary Fig. S1). In the hanging walls of the north-dipping Bardibas and Patu thrusts, up to six levels of fluvial terraces unconformably cap folded, south-dipping, Mid-Siwalik strata[15,16]. Whereas the oldest terrace remnants (~7 kyr; ref. 17) rise ~80 m above the Ratu River, the youngest hanging-wall terrace surfaces are regionally at most 3–5 m higher than the seasonal river floodplains[7] (Supplementary Fig. S1 and Fig. 2), which suggests recent co-seismic uplift.

Twentieth century and previous events on the Sir river cliff

Where the Sir River crosses the Patu thrust (Figs 1 and 2), we found exceptionally well-preserved evidence of recent faulting. Refreshing 50 m of the ~15 m-high cliff along the river's eastern bank revealed four north-dipping thrusts (Fig. 3a). Three of them (F1, F3, F4), outlined by dark gouge, terminate upwards just below ground and truncate ~2 m-thick gravel/pebble strata. The youthfulness of faulting is also clear from the morphology of the ~26 m-high cumulative thrust escarpment orthogonal to the river-cut cliff. The main slope-break near the base of the escarpment coincides with the emergence of F3 (Fig. 2), which brings sheared Siwaliks on fluvial deposits and colluvium containing collapsed Siwalik blocks (Fig. 3a). The emergence of F1 corresponds to an eroded scarplet across the low-level terrace T2f (Figs 2 and 3). 120 m eastwards, a small hanging tributary incision is flanked by narrow terrace benches perched yet higher (T3h, T4h, Fig. 2). A flat, cobble-paved strath surface (T5h), ~30 m above the river (T0, T′0), caps the hanging wall.

Detailed logging and dating (Fig. 3) demonstrate the young age of terrace T2 and the occurrence of recent seismic events on F1. The 27° N-dipping F1 thrust zone emplaces a toe of Siwalik sandstones—part of the south limb of a fault propagation anticline, with deformed, vertical bedding—on several conglomerate units, whose fluvial origin is clear from pebbles imbricated by south-directed water-flow. The youngest sediments—U0, silty sands with thin, concave-upwards gravel beds—fill a currently active rill channel at the foot of the eroded scarplet and seal the shallowest F1 splays (Fig. 3). The channel, in which one charcoal fragment yielded a modern ^{14}C age (Supplementary Table S1), postdates the

[1]National Seismic Center, Department of Mines and Geology, Lainchaur, Kathmandu, Nepal, [2]CEA, DAM, DIF, F-91297 Arpajon, France, [3]Univ. Paris Diderot, UMR 7154 CNRS, F-75005 Paris, France, [4]Earth Observatory of Singapore, Nanyang Technological University, Singapore 639798, Singapore.
*e-mail: Laurent.bollinger@cea.fr.

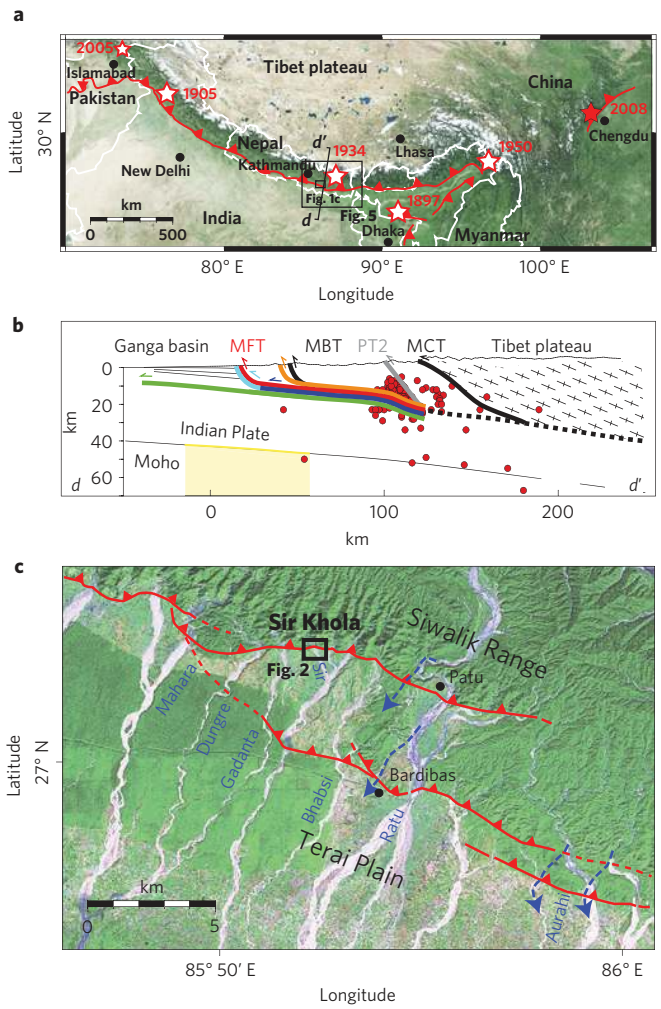

Figure 1 | Great earthquakes along Main Himalayan Thrust (MHT–MFT). **a**, Large open stars: great Himalayan earthquakes since 1895. Other stars: epicenters of 12 May 2008, $M \sim 8$, Wenchuan and 08 October 2005, $M \sim 7.5$, Muzzaffarabad earthquakes[1,3,4]. Red lines: MFT and other large thrusts. Boxes: locations of Figs 1c and 5. **b**, Coloured lines (section dd') show fault rupture scenarios and source sizes proposed for different events[10,12,13], mostly of thrust type. Small red circles: $1 < M_L < 5$ earthquakes, mostly in mid-crustal ramp swarm[26]. **c**, Map, superimposed on Landsat TM image, of right-stepping MFT strands (red) between Mahara and Aurahi rivers. Dashed blue lines with arrows are channels abandoned owing to east-directed, thrust-driven deviation of rivers.

topmost T2f deposits. These are mostly unconsolidated, beige/grey, clast-supported conglomerates with rounded pebbles/cobbles in a sandy/silty matrix (U2–U3), capped by a wedge of soft overbank and colluvial wash (U1), (Supplementary Section S1b). Six detrital charcoal fragments in the three T2 units, on the footwall and hanging wall, yielded consistent calibrated ^{14}C ages, ranging from AD 1490 to 1960 (Supplementary Table S1 and Fig. 3). The T2 conglomerates were thus emplaced by the river between the sixteenth and early twentieth centuries, before the hanging wall strath terrace T2h, now 4–5 m above river, was uplifted by ~3 m of co-seismic slip on the uppermost F1 splays (Fig. 3b,c). That only one deposit, a modern channel fill, caps F1 and U1, suggests that this ultimate F1 event must have been as recent as permitted by historical records. That the most recent, 15 January 1934, Bihar–Nepal earthquake was also the largest ($M_w \sim 8.2$) capable of generating a displacement of this size at this location implies that the Sir river-cut exposes the hitherto elusive surface rupture of that earthquake (Supplementary Section S1c). All Bayesian scenarios taking into account subsets of the U0–U3 sample ages yield age intervals that include 1934 at the 95.4% level (Supplementary Section S2 and Fig. S3A,B). The truncation of the U1–3 deposits beneath F3 (Fig. 3a) implies additional slip (≤2 m) on that thrust in 1934.

The T2f deposits overlie a lower F1 splay that cuts two underlying units: U4, a layer of poorly consolidated gravel/pebble conglomerate with sandy matrix, and U5, composed of thin, fine gravels interbedded with light-beige sand/silt lenses up to 20 cm thick. The sharply folded base of U5 in turn caps the lowest visible splay of F1, which truncates all units below: U6–10, mostly indurated, rusty-brown (oxidized), clast-supported pebble/cobble conglomerates, with clear channel sub-structures and erosional contacts (Fig. 3c). The most frontal thrust on the Sir river-cut thus bears evidence for three seismic events (Fig. 3 and Supplementary Fig. S2). The lenses of sheared conglomerates between the three main thrust-splays and stronger drag folding of the lowermost footwall units (Fig. 3c) corroborate increasing slip with depth, but removal by fluvial abrasion of all but the youngest strath deposits on the hanging wall precludes estimating the vertical throw related to the two oldest earthquakes. The missing stratigraphic section, due to footwall channel incision (bases of U4 and U6), also makes it difficult to constrain the timing and number of old events. Nevertheless, the ages in U3 suggest a penultimate event (E2) before the nineteenth century, and three consistent calibrated ^{14}C ages in U5 (1450–1130 BC, Fig. 3c and Supplementary Table S1) imply one other event (E3) before roughly 1130 BC. E3 might have also activated thrust F4, cutting and further uplifting the hanging-wall strath-terrace (1880–1630 BC) perched ~10 m above river beneath that thrust (Fig. 3a). That U5 in the footwall stands only ~1 m above the present riverbed implies little net fluvial incision in the past 3,500 years (<0.3 mm yr^{-1}). The local uplift rate of the hanging wall across the four thrusts, by contrast, is probably at least 3.5 mm yr^{-1}.

Evidence for the AD 1255 earthquake in the Sir trench

The 43 m-long, 5 m-deep trench we excavated on the east bank of the Sir River (M-Tr, Fig. 2) exposed two shallow-dipping thrusts (F1t and F3t, Fig. 4). Both are clear lateral equivalents of F1 and F3 on the river-cut (Figs 2–4), ~30 m westwards, but the stratigraphic units unearthed are somewhat different.

F3t emplaces a brecciated 'toe' of Siwalik siltstones (Siw), with cracks filled by red-brown clays, on a fluvial conglomerate sequence (U10t–U11t–U12t). This toe is buried under stacked colluvial wedges (U4t–U5t, U7t–U8t–U9t) with bases on flat sand layers (U3t, U6t) and apexes on the steep toe face (Fig. 4). They mix pebbles derived from terraces perched upslope with Siwalik fragments in a clay/silt matrix, implying collapse of the main escarpment's south face. The greater abundance and size of fragments at the base of the four lowermost wedges confirms sourcing from a 4 to 5 m-high free-face of heaved Siwaliks. The well stratified, finely laminated U6t sands, which incorporate organic-rich clay layers, probably filled a channel along the escarpment base at the time of collapse (Fig. 4).

F1t, a N117 ± 10° E-striking, 19 ± 2° N-dipping, multi-splay thrust south of the main escarpment (as F1 on the river-cut) emplaces U10t–U11t–U12t on a similar fluvial sequence (U13t–U14t–U15t), (Fig. 4). The three corresponding units in these two sequences (U10t and U13t: light-coloured, unconsolidated pebble and gravel beds; U11t and U14t: more consolidated, poorly sorted conglomerates with slightly oxidized pebbles/cobbles containing metric lenses of beige sands; U12t and U15t: well indurated and stratified gravel/pebble conglomerates, with well oxidized, rust-coloured horizons) are so alike that we interpret them to have been duplicated by thrusting. Despite irregular channeling, the

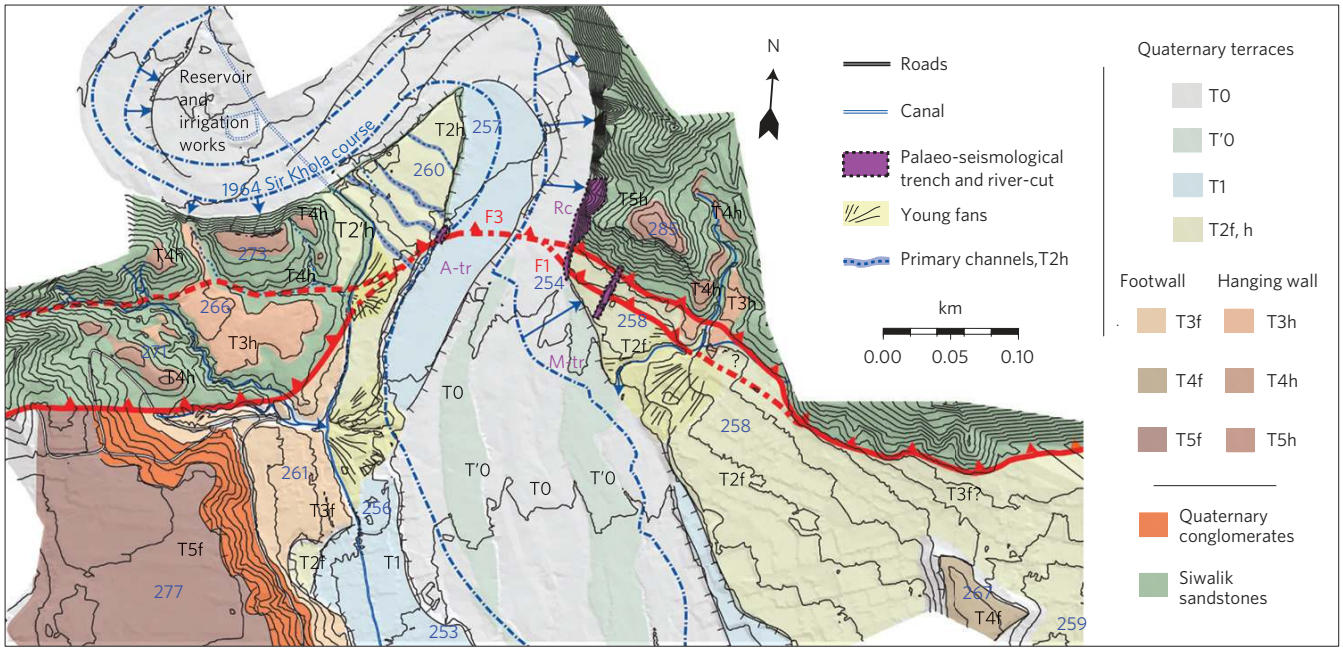

Figure 2 | Patu Thrust at Sir River site. Neotectonic/geomorphic map of the thrust trace (red, dashed where hidden or inferred) is superimposed on Total-Station/TLS Digital Elevation Model. Spacing of elevation contours is 2 m. Bold symbols (with question marks where inferred) and blue numbers are terrace names and altitudes (m) above sea level. Rc, M-Tr, and A-Tr are locations of river-cut, main and auxiliary palaeo-seismological trenches (violet). Blue dash-dotted lines and arrows show limits of the river channel in 1964 and the extent of lateral cutting since 1964, respectively.

conglomerate beds strike ~N110 ± 20° E and dip ~15 ± 10° N on average. The F1t splays are marked by aligned flat pebbles and thin oxidized gravel layers. The lowest splay, adjacent to a small footwall trough filled by fine sands, appears to have raised the top of U12t by at least 30–40 cm. Abrasion of U10t–U11t–U12t and the negligible angle with bedding preclude constraining slip amounts across F1t, although U13t extends at least 8 m beneath this thrust (Fig. 4). The last slip increment on F1t occurred recently because it is sealed only by superficial colluvial/overbank wash (U1t, U2t: silts with rare, isolated small pebbles and colluvium). These uppermost deposits, beneath the top soil, mantle the escarpment slope base and T2h terrace surface. One more unit (U3t: massive sands) fills twin channels beneath U2t.

Thirteen ^{14}C dates of detrital charcoal samples (Fig. 4 and Supplementary Table S1) place limits on the ages of the units. One date in a U11t sand lens (AD 570–665) implies that it was deposited in the seventh century AD, between the emplacements of U3 and U5 on the river-cut (Fig. 3c), as the river was flowing east along the F3t escarpment. Sometime after the seventh century AD, the Siwaliks were thrust onto the U10t conglomerates by one earthquake on F3t. The U6t sand layers and gravity-collapse wedges above were emplaced in the wake of this event (Fig. 4). Four ages in U6t indicate that the sands were deposited in the thirteenth–fourteenth centuries, which loosely brackets the earthquake occurrence to have been between about AD 700 and 1300. It seems probable, however, that the channel developed at the foot of the scarp soon after the earthquake, like the post-1934 U0 rill-channel on the river-cut. Thus, as corroborated by the Bayesian analysis of the U5t–U6t–U7t charcoal ages (Methods, Oxcal modelling, Supplementary Fig. S3C), we interpret the channel and collapse wedges to have been consequences of the devastating historical earthquake of 7 June 1255. An event in the eleventh century AD, as that inferred elsewhere in eastern Nepal[7,8], would not fit the age data as well. Finally, the two detrital charcoal ages (AD1520–1960) in the U1t silts that seal the tip of F1t (Supplementary Table S1 and Fig. 4) are consistent with a last event on F1t occurring in the first half of the twentieth century, as on the river-cut. The Oxcal modelling (Methods, Supplementary Fig. S2C) further supports the inference that it was the 1934 Bihar–Nepal earthquake.

Rupture length and return time of $M > 8$ events in Nepal

Our findings at the Sir River site therefore imply that two surface ruptures, each with plausibly about 4–5 m of throw, formed on splays of the Patu thrust during both the 1934 Bihar–Nepal earthquake and the catastrophic AD 1255 event, which killed 30% of the population of Kathmandu, including King Abhaya Malla[18]. An interval of 679 years would thus have elapsed between the last two great, surface-breaking MFT earthquakes in eastern Nepal.

Twenty five kilometres east of the Sir Valley, ^{14}C dated, <300 years-old hanging-wall terraces uplifted at least 4–6 m above river-beds where footwall incision is small, are observed in the Charnath river catchment[16]. Farther east, similarly uplifted hanging-wall terraces and ~5 m-high free-faced scarps are visible along the MFT all the way to the Sardu River in Dharan (Supplementary Fig. S3 and Fig. 5). Hence we infer that the 1934 Bihar–Nepal earthquake ruptured the MFT from at least 85° 52′ to 87° 17′ E, a minimum distance of ~150 km (Fig. 5 and Supplementary Section S3b). Such a rupture would fall within the 1934 MSK64 (Mercalli–Sponheur–Karnik, 1964). isoseismal VIII contour (ref. 19, reassessed in refs 20,21), and would lie due SSW of the event's relocated hypocenter[22] approximately 50 km South–SouthEast of Mt Everest (Fig. 5). Although estimated source parameters for the 1934 earthquake vary by factors of 2–4 (refs 20–22), a minimum seismic moment of 1.81×10^{20} N m (ref. 20) would be consistent with an average slip of ~5 m on a flat, 150×85 km^2 thrust patch[22], close to the initially proposed patch of 200×100 km^2 (ref. 19). In keeping with such values, our measurements at the Sir, Charnath and Sardu river sites suggest that a large fraction of the slip would have reached the surface. Concurrently, the Himalayan interseismic convergence rates (16–20 mm yr^{-1}) derived from either Global Positioning System or geomorphic studies[10,11,23–25], would imply a shortening deficit of ~12 ± 2 m in 679 years. This would result in a cumulative vertical co-seismic

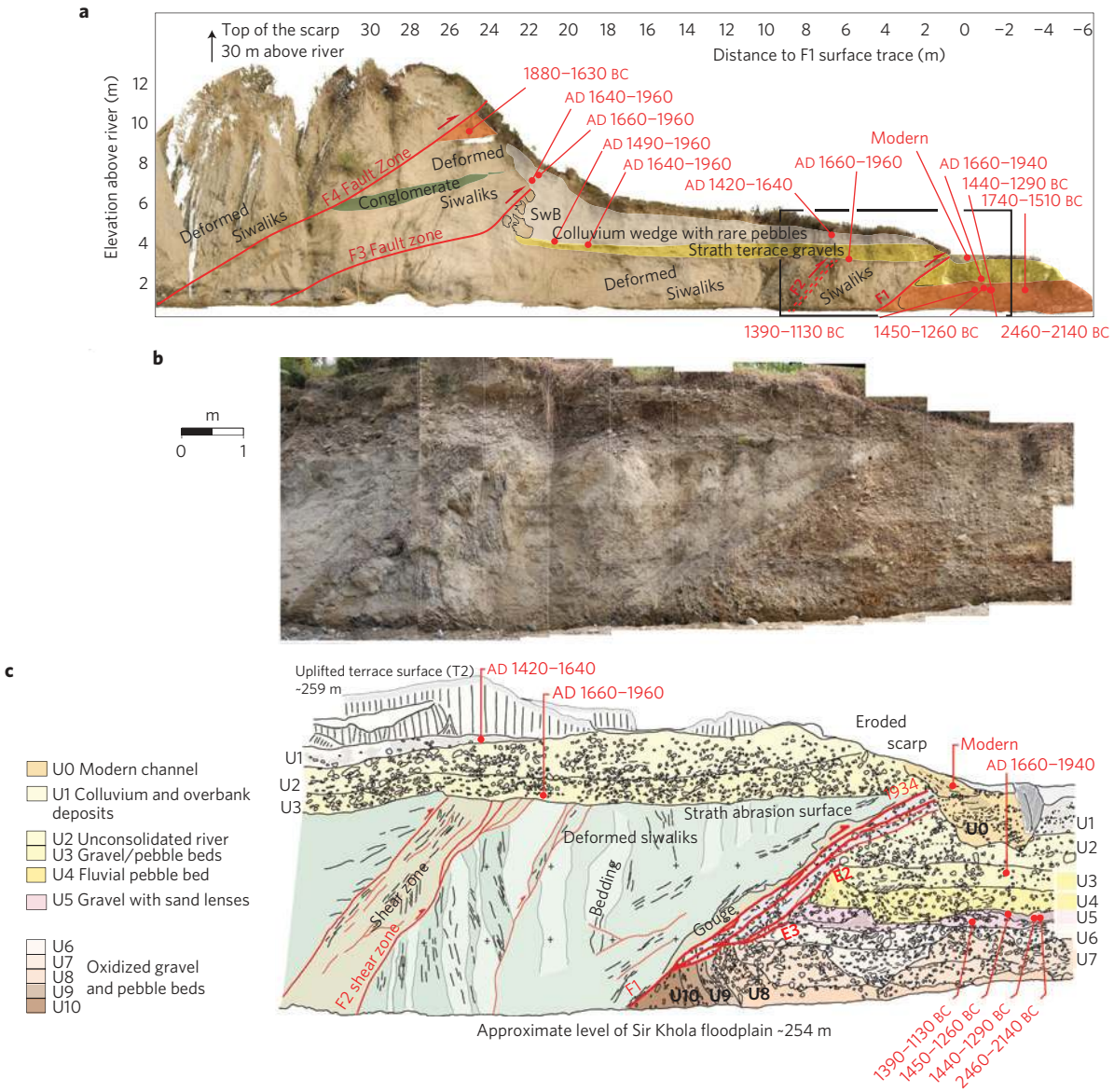

Figure 3 | Photo-mosaics and palaeo-seismological logs of Sir river-cut. a, Projection, on the vertical plane parallel to the cliff azimuth, of TLS Digital Elevation Model (DEM) and co-referenced mosaic of the entire refreshed face, gridded in metres. Four main thrusts are red; young and older terrace deposits are yellow and orange, respectively; mid-Siwalik conglomerate bed is green; colluvial/overbank wedge is beige; SwB are collapsed Siwalik blocks. Dots with numbers indicate the locations and 2σ calibrated calendric ages of 14 detrital charcoal samples. **b**, Photo-mosaic of river-cut front (box in **a**). A higher resolution zoom of the central part is shown in Supplementary Fig. S2. **c**, Detailed log of **b** as described in the text.

throw on the order of 4–5 m on superficial MFT splays dipping 18–22° N, roughly as observed for F1/F1t + F3/F3t on the east bank of the Sir River.

The seismic cycle scenario suggested by the Sir Valley outcrops is thus quite different from that inferred in the Mahara Valley from ~17 m of surface slip and ~8 m of vertical throw, which was attributed to only one very large event since AD 700 (ref. 7). Our results favour the simplest Himalayan deformation model (Fig. 1a, inset, red), in which most of the inter-seismic elastic loading south of the ramp plunging under the high range is relaxed during $M > 8.2$ earthquakes by co- and post-seismic slip on the Main Himalayan Thrust (MHT) flat beneath the Lesser Himalayas, transferring most of the shortening to the emergent MFT at the Siwalik Range front[25,26].

In hindsight, perhaps it is not surprising that the primary Bihar–Nepal earthquake rupture was not found earlier. In 1934, the remote Terai edge was densely forested and sparsely inhabited owing to endemic malaria. Damage caused by focused SmS seismic phase is a well-known seismic phase arrivals[21] and widespread liquefaction diverted attention to the Ganges Plain. That the MFT, then crossed by only two roads, was active had not yet been clearly established. Thrusts tend to produce discontinuous, stepping and festooned 'fold-scarps'[2], which are less clear than normal or strike-slip fault breaks. Most importantly, monsoon floods may destroy co-seismic surface scarps and stratigraphic records in just a few seasons. In less than 50 years, for instance, the Sir River laterally eroded its banks by 15–40 m (Fig. 2). Nevertheless, the rare exposure it spared raises hope that more tell-tale outcrops might be found and that the surface ruptures of other reputedly 'blind' Himalayan great earthquakes might exist. A more systematic 'search-and-find' strategy would open the way to more productive palaeo-seismological research and to a better assessment of Himalayan seismic hazard. Equally important, finding such ruptures would improve our understanding of the

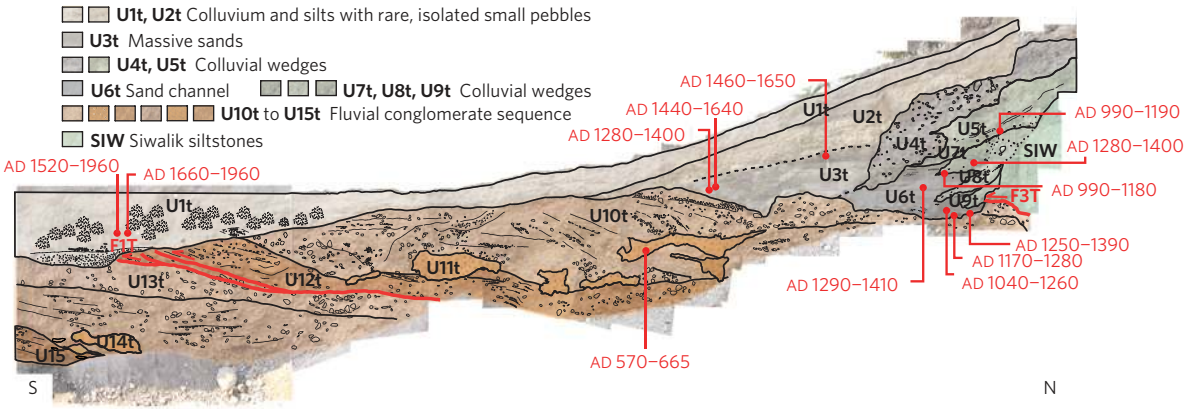

Figure 4 | Simplified log of main trench on the east bank of the Sir River. M-Tr, location on Fig. 2. Only the northern half (~26 m) of the trench west wall is shown, with thrusts F1t and F3t in red. Also in red are the positions and 2σ calibrated calendric ages of 13 detrital charcoals collected on the west wall. Symbols of units described in text are in bold.

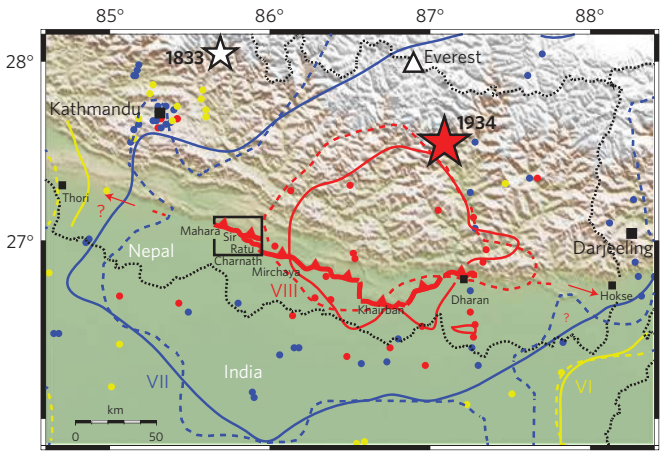

Figure 5 | 1934 surface break. Inferred co-seismic rupture (thick red line), superimposed on SRTM topography. Red and white stars are instrumental and macroseismic epicenters of 1934 (ref. 21) and 1833 (ref. 15) events, respectively (Supplementary Section S1c). Thin continuous and dashed coloured lines with roman numbers are 1934 macroseismic isoseismals (MSK64), respectively from ref. 19 and ref. 15. Dotted black lines are borders. Black box, location of Fig. 1c. Red arrows with question marks point to the maximum rupture extent (Supplementary Section S3b).

seismic behaviour of the MHT–MFT, and of the mechanics of plate-boundary mega-thrusts in general.

Methods

Surveying and logging. In the field, we used 1964 aerial photographs, submetric resolution Ikonos and Geoeye-1 satellite images, photographs taken during a dedicated helicopter survey, and recent, 1/25,000 scale, topographic sheets as a basis for our geologic/geomorphic mapping and study of the tectonic landscape evolution with time. We used Total-Station leveling and Terrestrial Lidar Scanning (TLS; Riegl VZ 400), with three-dimensional precisions of 30 and 2 cm, respectively, to survey the local tectonic/fluvial geomorphology and log the structure of newly excavated or refreshed exposures (Figs 2–4 and Supplementary Section S1a).

^{14}C dating. We dated 14 and 13 of the charcoal samples collected in fluvial and colluvial deposits along the river-cut face and west wall of the main trench, respectively. The prepared charcoal fragments were analysed by Accelerator Mass Spectrometry at the SUERC radiocarbon dating laboratory in Glasgow. The results, with uncertainties, are listed in Supplementary Table S1. The total time span of the stratigraphic record sampled, calibrated with IntCal09 (ref. 27), extends roughly from 2500 BC to the present. The chronological sequence was further refined by introducing a priori information from stratigraphic relationships, using the Bayesian analysis approach of Oxcal 4.1 (ref. 28). The simplest deposition and rupturing scenarios tested for the river-cut exposure and the main palaeo-seismological trench are discussed below and shown in the Supplementary Fig. S3A–C).

Modelling the radiocarbon dating with Oxcal. On the river-cut, we tested three simple deposition scenarios.

In the first, we assume a sequence with three distinct deposition phases (Supplementary Fig. S3A). The earliest phase corresponds to the emplacement of the small sand lenses (U5) that contain charcoal samples SIR09-01, -03, -04, -11 and -15, on top of the indurated, oxidized, U6–10 footwall conglomerates; the second, to the deposition of the unconsolidated strath pebble beds (U2–U3, containing SIR08-11, -12, -26, and SIR09-13) on the footwall and hanging wall, assuming all four samples to have been emplaced in phase; and the latest, to the emplacement of the fine colluvium and overbank deposits (U1) in which SK10-05 and -07 were found. The U2–U3 deposits were offset by slip on F1 during earthquake E1, followed by deposition of the overbank/colluvial wedge (U1). Within U1, detrital charcoal fragments are interpreted to be reworked (for example, SIR09-17, Supplementary Table S1) down from uplifted older units on the main escarpment slope, with SK10-05 and -07 young enough, however, to postdate E1. Although over-constrained, this model does predict, at the 95.4% level, an earthquake date between AD 1730 and 1940, including 1934 (Supplementary Fig. S3A, Darker Probability Density Function (PDF), Supplementary Fig. S3B, bold PDF curve).

In the second scenario, we assume an overall deposition sequence similar to the first, but infer that the four U2–3 charcoals have been emplaced in sequence as a function of their relative depths. The corresponding Oxcal4.1 model predicts an almost identical date range, between AD1720 and 1940, also including 1934, at the 95.4% level (Supplementary Fig. S3B, dashed PDF curve).

In the third scenario, we exclude all the U1 reworked samples and include the calibrated age of the modern, 'post-bomb' sample[29] (SIR08-03) in channel U0, which truncates F1 and therefore must postdate E1 (Fig. 3c). The corresponding Oxcal4.1 model yields a PDF (dot–dashed curve on fig. S3B) with an age range between AD 1795 and 1963 at the 95.4% level.

All three scenarios thus yield consistent modelled date ranges that are compatible with event E1 being the 15 January 1934, $M \sim 8.1$, Bihar–Nepal earthquake. Note, however, that none of the models excludes the 26 August 1833, $M \sim 7.6$ earthquake (Supplementary Section S1c).

For the main trench, we present here the simplest testable Bayesian model, in which we assume that all the detrital charcoals are in stratigraphic order, from U11t below to U1t on top, irrespective of whether they were collected in fluvial, overbank, colluvial or collapse deposits (Supplementary Table S1 and Fig. 4). This excludes samples SIR08-22 and -39 in U5t and U7t, which are clearly reworked, leaving only 11 ages to constrain the model (Supplementary Fig. S3).

The trench stratigraphy and ages suggest a scenario in which a first earthquake (event E2, on F3t) occurs after deposition of fluvial unit U11t (AD 570–665) and during deposition of U6t, slightly before the collapse of wedge U7t. Then a second earthquake (event E1, on F1t) occurs before deposition of U1t (AD 1520–1960). According to the individually calibrated age of SIR08-20 (Supplementary Table S1) at the very base of U6t (light grey, Supplementary Fig. S3C), E2 cannot be earlier than around AD 1250. Similarly, given the further age constraints on the nearby river-cut, it is likely that E1 ruptured F1t after deposition of U3, hence in the twentieth century (Fig. 3c).

Using Oxcal4.1, we therefore test whether the great historical earthquakes of 07 June 1255 and 15 January 1934 can correspond to E2 and E1, respectively. As shown on Supplementary Fig. S3C (dark grey distributions), the modelled PDFs of

the 11 stratigraphically ordered trench samples indeed support this simple surface faulting scenario, implying that the 1934 earthquake, like the 1255 event, ruptured the Patu thrust after 679 years of quiescence.

Received 29 June 2012; accepted 13 November 2012; published online 16 December 2012

References

1. Avouac, J. P. *et al.* The 2005 Mw 7.6 Kashmir earthquake: Sub-pixel correlation of ASTER images and seismic waveforms analysis. *Earth Planet. Sci. Lett.* **249,** 514–528 (2006).
2. Chen, W. S. *et al.* Paleoseismic evidence for coseismic growth-fold in the 1999 Chichi earthquake and earlier earthquakes, central Taiwan. *J. Asian Earth Sci.* **31,** 204–213 (2007).
3. Liu-Zeng, J. *et al.* Surficial slip and rupture geometry on the Beichuan fault near Hongkou during the Mw 7.9 Wenchuan earthquake, China. *Bull. Seismol. Soc. Am.* **100,** 2615–2650 (2010).
4. Xu, X. W. *et al.* Coseismic reverse- and oblique-slip surface faulting generated by the 2008 Mw 7.9 Wenchuan earthquake, China. *Geology* **37,** 515–518 (2009).
5. Yeats, R. S. *et al.* The Himalayan frontal fault system. *Ann. Tectonicae* **6,** 85–98 (1992).
6. Nakata, T. in *Tectonics of the Western Himalayas* (eds L. L., Malinconico & Lillie, R.) 243–264 (Geol. Soc. of America, spec. Paper, 1989).
7. Lavé, J. *et al.* Evidence for a great medieval earthquake (AD~1100) in the Central Himalayas of Nepal. *Science* **307,** 1302–1305 (2005).
8. Kumar, S. G. *et al.* Paleoseismological evidence of surface faulting along the northeastern Himalayan front, India: Timing, size, and spatial extent of great earthquakes. *J. Geophys. Res.* **115,** B12422 (2010).
9. Kumar, S. *et al.* Paleoseismic evidence of great surface rupture earthquakes along the Indian Himalaya. *J. Geophys. Res.* **111,** B03304 (2006).
10. Bilham, R., Gaur, V. K. & Molnar, P. Earthquakes—Himalayan seismic hazard. *Science* **293,** 1442–1444 (2001).
11. Ader, T. *et al.* Convergence rate across the Nepal Himalaya and interseismic coupling on the Main Himalayan Thrust: Implications for seismic hazard. *J. Geophys. Res.* **117,** B04403 (2012).
12. Feldl, N. & Bilham, R. Great himalayan earthquakes and the Tibetan plateau. *Nature* **444,** 165–170 (2006).
13. Kayal, J. R. Himalayan tectonic model and the great earthquakes: An appraisal. *Nature Hazards Risk* **1,** 51–67 (2010).
14. Seeber, L. & Armbruster, J. in *Earthquake Prediction: An International Review* (eds D. W., Simpson & P. G., Richards) 259–277 (Maurice Ewing Series Vol. 4, Am. Geophys. Un., 1981).
15. Delcailleau, B. Les Siwaliks du Népal oriental. *Presses du CNRS* (Editions du Centre National de la Recherche Scientifique, 1992).
16. Sapkota, S. N. *Surface Rupture of the 1934 Bihar–Nepal Earthquake: Implications for Seismic Hazard in Nepal Himalaya* (IPGP, 2011) unpublished PhD thesis.
17. Corvinus, G. Prehistoric Cultures in Nepal. *Harrassoeitz Verlag Wiesbaden* **1,** 239–246 (2007).
18. Pant, M. R. A step toward a historical seismicity of Nepal. *Adarsa* **2,** 29–60 (2002).
19. Pandey, M. R. & Molnar, P. The distribution of intensity of the Bihar–Nepal earthquake of 15 January 1934 and bounds on the extent of the rupture zone. *J. Nepal Geol. Soc.* **5,** 22–44 (1988).
20. Ambraseys, N. N. & Douglas, J. Magnitude calibration of north Indian earthquakes. *Geophys. J. Int.* **159,** 165–206 (2004).
21. Hough, S. E. & Bilham, R. Site response of the Ganges basin inferred from re-evaluated macroseismic observations from the 1897 Shillong, 1905 Kangra, and 1934 Nepal earthquakes. *J. Earth Syst. Sci.* **117,** 773–782 (2008).
22. Chen, W. P. & Molnar, P. Seismic moments of major earthquakes and the average rate of slip in Central Asia. *J. Geophys. Res.* **82,** 2945–2969 (1977).
23. Jouanne, F. *et al.* Current shortening across the Himalayas of Nepal. *Geophys. J. Int.* **157,** 1–14 (2004).
24. Bettinelli, P. *et al.* Plate motion of India and Interseismic Strain in the Nepal Himalaya from GPS and DORIS measurements. *J. Geod.* **80,** 567–589 (2006).
25. Lavé, J. & Avouac, J-P. Active folding of fluvial terraces across the Siwaliks Hills, Himalayas of Central Nepal. *J. Geophys. Res.* **105,** 5735–5770 (2000).
26. Cattin, R. & Avouac, J-P. Modeling mountain building and the seismic cycle in the Himalaya of Nepal. *J. Geophys. Res.* **105,** 13389–13407 (2000).
27. Reimer, P. J. *et al.* IntCal09 and Marine09 radio'carbon age calibration curves, 0–50,000 years cal BP. *Radiocarbon* **51,** 1111–1150 (2009).
28. Bronk Ramsey, C. Deposition models for chronological records. *Quat. Sci. Rev.* **27,** 42–60 (2008).
29. Hua, Q. & Barbetti, M. Review of tropospheric bomb C-14 data for carbon cycle modeling and age calibration purposes. *Radiocarbon* **46,** 1273–1298 (2004).

Acknowledgements

The research was principally funded by EOS (NTU, Singapore), with contributions from CEA/DASE and Project PAKSIS (ANR Cattel) in France. We thank M. Goh (EOS) for technical assistance with the Lidar data acquisition and processing, N. Shrestha (Kathmandu) for total station topographic surveying, and G. Cook (SUERC Radiocarbon Dating Laboratory, University of Glasgow, UK) for the charcoal samples analyses. We are grateful to the young men of Cheru for refreshing and cleaning the river-cut cliff and trench walls. We also thank the Department of Mines and Geology in Kathmandu, Nepal, for constant logistical support, and F. Perrier and B. N. Upreti for excellent guidance during a first exploratory field trip. We are particularly indebted to F. Perrier for having inspired this study from the start. S. Wesnousky and T. Rockwell provided thoughtful, constructive comments that helped improve the original manuscript. This is EOS/NTU contribution number 40.

Author contributions

The data and results presented in this paper are part of Som Sapkota's PhD thesis (Institut de Physique du Globe, Paris, France). P.T. led the project. All authors contributed to the fieldwork and sampling. S.N.S., Y.K., L.B. and P.T. contributed equally to the logging and interpretation of the river-cut face and trench wall. S.N.S., Y.K. and P.T. drafted the original logs shown on Figs 3 and 4, and P.T., L.B. and S.N.S., the original maps of Figs 1 and 2. L.B. directed the dating effort, performed the Oxcal modelling, and drafted the final versions of the figures. P.T., L.B. and S.N.S. wrote the paper.

Additional information

Supplementary information is available in the online version of the paper. Reprints and permissions information is available online at www.nature.com/reprints. Correspondence and requests for materials should be addressed to L.B.

Competing financial interests

The authors declare no competing financial interests.